Preprints.org

Article

Sinorhizobium meliloti GR4 Produces Chromosomal- and pSymA-Encoded Type IVc Pili That Influence the Interaction With Alfalfa Plants

Cristina Carvia-Hermoso , Virginia Cuéllar , Lydia M. Bernabéu-Roda , Pieter Van Dillewijn [*] , María J. Soto [*]

Article

Sinorhizobium meliloti GR4 Produces Chromosomal- and pSymA-Encoded Type IVc Pili that Influence the Interaction with Alfalfa Plants

Cristina Carvia-Hermoso [1]**, Virginia Cuéllar** [1]**, Lydia M. Bernabéu-Roda** [1]**,
Pieter van Dillewijn** [1,]*** and María José Soto** [1,]***

[1] Department of Biotechnology and Environmental Protection, Estación Experimental del Zaidín, CSIC,
     18008 Granada, Spain: cristina.carvia@eez.csic.es (C.C.-H.); virginia.cuellar@eez.csic.es (V.C.);
     lydia.bernabeu@eez.csic.es (L.M.B.-R.); pieter.vandillewijn@eez.csic.es (P.v.D.); mariajose.soto@eez.csic.es
     (M.J.S.)
* Correspondence: P.v.D. pieter.vandillewijn@eez.csic.es, Tel: + 34 958526450; M.J.S.
     mariajose.soto@eez.csic.es, Tel: + 34 958526477

Abstract: Type IVc Pili (T4cP), also known as Tad or Flp pili, are long thin microbial filaments, which are made-up of small-sized pilins. These appendages serve different functions in bacteria including attachment, biofilm formation, surface sensing, motility, and host colonization. Despite their relevant role in diverse microbial lifestyles, knowledge about T4cP in bacteria that establish symbiosis with legumes, collectively referred to as rhizobia, is still limited. *Sinorhizobium meliloti* contains two clusters of T4cP-related genes: *flp-1* and *flp-2*, which are located on the chromosome and pSymA megaplasmid, respectively. Bundle-forming pili associated to *flp-1* have been involved in competitive nodulation of alfalfa plants but the role of *flp-2* remains elusive. In this work, we have performed a comprehensive bioinformatic analyses of T4cP genes in the highly competitive *S. meliloti* strain GR4 and investigated the role of its *flp* clusters in pilus biogenesis, motility and in the interaction with alfalfa. Single and double *flp* cluster mutants were constructed in the wild-type genetic background as well as in a flagellaless derivative strain. Our data demonstrate that both chromosomal and pSymA *flp* clusters are functional in pili biogenesis, and contribute to surface translocation and nodule formation efficiency of GR4. In this strain, the presence of *flp-1* in the absence of *flp-2* reduces competitiveness for nodule occupation.

Keywords: Tad/Flp pili; *Rhizobium*; plant colonization; nodulation; competitive ability

1. Introduction

     Sinorhizobium meliloti is an alpha-proteobacterium that can live as a saprophyte in the soil but can also establish nitrogen-fixing symbiosis with alfalfa plants [1]. Successful establishment of this symbiosis results in the formation of root nodules, which are infected by bacteria that fix atmospheric dinitrogen into ammonia for direct use by the plant. The progress of this interaction entails different phases and a sophisticated molecular dialogue between the legume host and the rhizobial microsymbiont [1–3]. An early and crucial step for the establishment of symbiosis is the bacterial colonization of plant roots, a process that is initiated with the motility of rhizobia towards the plant root and is followed by bacterial attachment to the root surface and the development of a microbial community or biofilm [4,5].

     Rhizobial motility is not essential for nodulation or nitrogen fixation but is an important trait for root colonization and infection, which eventually could influence nodulation efficiency and competitiveness [6–11]. *S. meliloti* can move using different mechanisms. Movement of bacteria in aqueous environments or swimming is absolutely reliant on flagellar action whereas translocation of the alfalfa microsymbiont over surfaces can be mediated by both flagella-dependent and –independent mechanisms [10,12–15]. Swarming is a flagella-driven type of motility characterized by the rapid and coordinated migration of cells across surfaces [16–18]. This motility has been described in *S. meliloti* [10,12,13] and in other rhizobia [19–22]. *S. meliloti* flagellaless strains can exhibit a mode

of surface spreading referred to as sliding [23]. In this case, bacterial movement is the result of expansive forces of cell growth together with the production of surfactants that reduce surface tension (e.g. exopolysaccharides and the amphiphilic siderophore rhizobactin 1021) [10,13]. Another flagella-independent mode of surface translocation described in many bacteria but not yet in rhizobia is twitching, which is mediated by the extension and retraction of type IV pili (T4P) [24,25]. Like flagella, T4P enable bacteria to not only move but also to attach to surfaces contributing to biofilm formation and host colonization [4,11].

T4P are long, flexible and elastic bacterial extracellular filaments, which are thinner than flagella and are made up of thousands of protein subunits called pilins [24,26–28]. These appendages have the peculiarity of being dynamic as rapid polymerization and depolymerization of pilin subunits carried out by a complex machinery permit pili to extend and contract. This characteristic is essential for the different functions associated with T4P [29].

The classification of T4P distinguishes three types: T4aP, T4bP, and the Tight Adherence (Tad) pili, also known as Flp (Fimbrial low-molecular-weight proteins) pili or T4cP [29,30]. One of the features that differentiates the different types of T4P is their major pilin sequences. Pilins of T4aP range between 150-175 amino acids, T4bP pilins are larger (180-200 amino acids) and T4cP are made up of small-sized pilins (50-80 amino acids) [29,31]. In addition, the genes required for T4aP biogenesis are numerous (more than 40) and are often scattered throughout the bacterial genome. In contrast, the synthesis of T4bP and T4cP requires a smaller number of genes (12-14) and they are usually grouped in a region, sometimes with genetic island characteristics [29].

The genes encoding dedicated proteins for polymerization and secretion of T4cP have a very specific and conserved genetic organization as is the case for the Tad system of *Aggregatibacter actinomycetemcomitans* (formerly *Actinobacillus actinomycetemcomitans* [32–36]), the *cpa* (*Caulobacter* pilus assembly) locus of *Caulobacter vibrioides* (formerly *Caulobacter crescentus* [37]), or the *ctp* (Cluster of type IV pili) locus of *Agrobacterium fabrum* C58 (formerly *Agrobacterium tumefaciens* C58 [38]) (Figure 1a). Before the major Flp pilin can be incorporated into the growing T4c pilus, it needs to be processed by a specific prepilin peptidase (TadV/CpaA/CtpB) that removes a leader sequence at a conserved glutamate and tyrosine containing Flp motif (GXXXXEY [34]). TadV also participates in the maturation of the TadE and TadF pseudopilins which share the conserved GXXXXEF sequence at their N-terminal but play an as yet unclear role in pilus biogenesis [35,39,40]. TadA/CpaF/CtpG is the cytosolic ATPase that catalyzes both the extension and retraction of pili with the help of the inner membrane platform proteins TadB/CpaG/CtpH and TadC/CpaH/CtpI [27]. TadZ/CpaE/CtpF is a docking protein for the Tad secretion system, which may help localize pili formation to the poles [40–42]. In diderms, T4cP pass through the outer membrane via the secretin RcpA/CpaC/CtpD, which requires the lipoprotein TadD/CpaO that functions as a pilotin enabling the assembly and correct insertion of the secretin into the outer membrane [40,43]. RcpB/CpaD/CtpE and RcpC/CpaB/CtpC probably form a complex with RcpA [36] and possibly are also important for the assembly and stability of the secretin complex [35].

Figure 1. Type IVc pili genes from different Gram negative bacteria. (**a**) The *tad/cpa/ctp* loci of *Aggregatibacter actinomycetemcomitans* CU1000N with gene names according to Kachlany et al. (2001) [34], of *Caulobacter vibrioides* NA1000 with gene names according to Skerker and Shapiro (2000) [37], Christen et al. (2016) [57], and Mignolet et al. (2018) [58], and of *Agrobacterium fabrum* C58 with gene names according to Wang et al., 2014 [38]. (**b**) Rhizobial Type IVc pili gene clusters and loci of *S. meliloti* GR4, *Sinorhizobium fredii* NGR234 [51], and *Bradyrhizobium diazoefficiens* USDA 110 with gene names according to Mongiardini et al. (2016) [50]. In the absence of assigned names, gene identifiers are used. In the case of *S. meliloti* GR4, assigned names and gene identifiers for *S. meliloti* Rm1021 were used for short word length. Similar colors indicate similar gene products by identity or assigned function. Dark grey arrows indicate hypothetical proteins putatively associated with pili assembly and light grey arrows hypothetical proteins or proteins annotated with non-pili related functions. The asterisk indicates the position of an additional IS*Rm22* element in the genome of *S. meliloti* Rm1021. ‡ BRC ID (https://www.bv-brc.org/).

T4cP genes are widely distributed amongst bacteria indicating that they confer significant adaptive advantages [29,35]. They have been involved in diverse functions such as surface sensing, motility, cell adhesion, formation of biofilm, host colonization, virulence, or even in bacterial predation [27,29,44]. Concerning the interaction with plant hosts, T4cP have been involved in the virulence of *Ralstonia solanacearum* and *Pectobacterium atrosepticum* [45,46]. In 'Candidatus Liberibacter asiaticus', the causal agent of citrus greening disease, Tad pili contribute to the colonization of the insect vector and therefore to disease propagation [47].

There is very little information on T4cP in rhizobia in general, and in *S. meliloti* in particular. A first indication for pilus like structures in rhizobia and their implication in attachment to roots was described in the soybean symbiont *Bradyrhizobium diazoefficiens* (formerly *Bradyrhizobium japonicum*) by Vesper and Bauer (1986) [48]. Information from genome sequencing is revealing that the majority of rhizobial species carry chromosomal gene clusters putatively encoding T4cP, and in many cases additional truncated clusters are also found [11,49–53]. In *B. diazoefficiens* USDA 110, additional *tadGEF* genes were found away from the two main T4cP clusters of *tad* and *cpa* genes and their loss affected adhesion to soybean roots and caused delayed root infection [50]. In *S. meliloti* Rm1021, two

clusters of genes that encode different components of T4cP have been identified [53]. The *flp-1* cluster is located on the chromosome while the second cluster, *flp-2*, is located on the symbiotic megaplasmid pSymA and appears to be truncated in Rm1021. Deletion of *pilA1* that encodes the major pilin of the *flp-1* cluster abolishes pili formation and reduces the competitiveness ability of Rm1021 to nodulate alfalfa [53]. However, data available up to now do not implicate these appendages with any type of motility in *S. meliloti* [53] and the role of each *flp* cluster in the nodulation process still remains unclear.

S. meliloti GR4 is a highly competitive strain for nodulation of alfalfa [54,55] that exhibits increased biofilm formation on both abiotic and root surfaces compared to Rm1021 [9]. In this work, we have performed a comprehensive bioinformatic analyses of T4cP genes in GR4 and investigated the role of its *flp-1* and *flp-2* clusters in pilus biogenesis, motility and in the interaction with alfalfa plants by using single and double *flp* cluster deletion mutants. Our data demonstrate that both chromosomal and pSymA *flp* clusters are functional in pili biogenesis. These appendages contribute to the surface translocation exhibited by *S. meliloti* GR4 and influence its symbiotic fitness.

2. Results

2.1. In silico analyses of Type IVc Pili (T4cP) genes of S. meliloti GR4

To identify T4cP-related genes in *S. meliloti* strain GR4, its genome was scanned for loci similar to *tad/cpa/ctp* genes (Figure 1, Table 1). We found a total of 29 genes with 16 of them located on the chromosome and 13 on the pSymA megaplasmid. All 29 T4cP-related genes found in GR4 have their corresponding orthologues in the reference strain Rm1021 with sequence identities higher than 98.4%. Therefore, for simplicity, in the text we will refer to the different T4cP genes using the nomenclature of Rm1021 (https://iant.toulouse.inra.fr/bacteria/annotation/cgi/rhime.cgi). In the two *S. meliloti* strains, GR4 and Rm1021, the majority of the T4cP genes are organized in two clusters: *flp-1* located on the chromosome and *flp-2* on pSymA (Figure 1b). Additional orphan loci could be identified upstream from *flp-1* on the chromosome and a third locus carrying three T4cP genes is located on pSymA (Figure 1b).

The *flp-1* cluster shows a synteny very similar to that found in *C. vibrioides* and carries all of the genes needed to build a complete and functional T4cP apparatus (Figure 1, Figure 2a, Table 1). Indeed, the formation of bundle-forming pili has been associated to this chromosomal cluster in strain Rm1021 [53]. Two copies of the insertion sequence IS*Rm22* are present in the chromosomal *flp* cluster of Rm1021 [53] but in GR4 only one copy of this IS element exists (Figure 1b). Nine of the 13 genes in the *flp-1* cluster are organized in one operon [56], namely *pilA1* coding for the major Flp pilin; *cpaA1* that codes for the putative prepilin peptidase; *cpaB1*, *cpaC1* and *cpaD1* coding for components of the outer membrane secretin complex; *cpaE1* coding for a putative docking protein of the secretion system; *cpaF1* encoding the pilus assembly ATPase; and *smc02821* and *smc02822*, orthologues of *cpaG* and *cpaH* genes [57], that code for inner membrane platform proteins.

The locus *smc02824*, located downstream of the IS*Rm22* element in GR4, codes for a tetratricopeptide repeat (TPR)-containing protein homologous to CpaO. Upstream of *pilA1*, the locus *smc04115* and the operon formed by *smc04117* and *smc04118* are found. These genes are *cpaI*, *cpaJ* and *cpaK* homologues coding for a CpaC-related secretion pathway protein, and TadE and TadF pseudopilins, respectively [57]. In addition, outside of the *flp-1* cluster, two additional chromosomal genes with putative roles in T4cP biogenesis were identified: *smc02446* and *smc03784* (Figure 1b, Table 1). The 57 amino acid protein encoded by *smc02446* is annotated as an Flp pilin component that contains the characteristic Flp motif recognized by the prepilin peptidase, and is a paralogue of PilA1 (60% identity in 71% query coverage) and of the *flp-2*-encoded pilin PilA2 (64% identity in 43% query coverage) (Figure S1a). According to Schlüter et al. (2013) [56], *smc02446* is transcribed in an operon together with *smc02447* that codes for a hypothetical transmembrane protein of unknown function. Finally, the orphan *smc03784* gene codes for a transmembrane protein that exhibits 39.34% identity with *C. vibrioides* CpaM, a polar determinant suggested to affect the biogenesis of functional pili portals [57,58]. Both proteins, CpaM and SMc03784, contain a C-terminal domain of divergent

polysaccharide deacetylases involved in the removal of *N*-linked acetyl groups from cell wall polysaccharides.

Table 1. Percent amino acid sequence identities (in parenthesis) between the products of T4cP genes of *S. meliloti* GR4 and the closest orthologues of the *tad* genes of *A. actinomycetemcomitans* CU1000N (**Aa**), the *cpa* genes of *C. vibrioides* NA1000 (**Cv**), the *ctp* genes of *A. fabrum* C58 (**Af**), the *tad/cpa* genes of *B. diazoefficiens* USDA 110 (**Bd**), and the *tad/cpa* genes of *S. fredii* NGR234 (**Sf**).

Locus GR4/Rm1021	Description	Aa	Cv	Af	Bd	Sf
Chromosome *flp-1*						
C770_GR4Chr0141/*smc 04118*	CpaK-like pseudopilin		CpaK (25)		TadF (26)	NGR_c34610 (60)
C770_GR4Chr0142/*smc 04117*	CpaJ-like pseudopilin		CpaJ (32)		TadE (29)	NGR_c34620 (69)
C770_GR4Chr0143/*smc 04115*	CpaI-like putative pili related protein		CpaI (26)	Atu0226 (63)	Blr1444 (35)	NGR_c34630 (88)
C770_GR4Chr0144/*smc 04114* (*pilA1*)	Flp pilin subunit	Flp-2 (34)	PilA (51)	CtpA (76)	Bsr1550 (51)	NGR_c34640 (71)
C770_GR4Chr0145/*smc 04113* (*cpaA1*)	Putative prepilin peptidase	TadV (31% in 65aa stretch)	CpaA (37)	CtpB (52)	TadV (43)	NGR_c34650 (71)
C770_GR4Chr0146/*smc 04112* (*cpaB1*)	Component of the outer membrane secretin complex		CpaB (35)	CtpC (64)	Bll1440 (39)	NGR_c34660 (87)
C770_GR4Chr0147/*smc 04111** (*cpaC1*)	Component of the outer membrane secretin complex	RcpA (26)	CpaC (34)	CtpD (70)	RcpA (40)	NGR_c34670 (87)
C770_GR4Chr0148/*smc 04110* (*cpaD1*)	Component of the outer membrane secretin complex		CpaD (39)	CtpE (58)	Bll1438 (35)	NGR_c34680 (80)
C770_GR4Chr0149/*smc 04109* (*cpaE1*)	Putative docking protein of the secretion system	TadZ (23)	CpaE (47)	CtpF (71)	TadZ (49)	NGR_c34690 (87)
C770_GR4Chr0150/*smc 02820* (*cpaF1*)	Pilus assembly ATPase	TadA (50)	CpaF (72)	CtpG (81)	TadA (72)	NGR_c34700 (90)
C770_GR4Chr0151/*smc 02821*	CpaG-like putative inner membrane platform protein	TadB (22)	CpaG (42)	CtpH (64)	TadB Locus 1 (48)	NGR_c34710 (89)
C770_GR4Chr0152/*smc 02822*	CpaH-like putative inner membrane platform protein	TadC (21)	CpaH (48)	CtpI (69)	TadC Locus 1 (54)	NGR_c34720 (90)
C770_GR4Chr0153/*smc 04116* (TRm22)	Insertion sequence IS*Rm22*					
C770_GR4Chr0154/*smc 02824*	CpaO-like TPR containing protein		CpaO (37)	Atu0215 (66)	TadD Locus 1 (45)	NGR_c34740 (84)
Chromosomal orphan loci						
C770_GR4Chr2732/*smc 02446*	Flp pilin subunit	Flp-2 (35)	PilA (60)	CtpA (51)	Bsl4812 (51)	‡fig|394.7.peg.5 489 (60)
C770_GR4Chr2733/*smc 02447*	Hypothetical protein			Atu3515 (52)		NGR_c26670 (95)

Locus	Function					
C770_GR4Chr3249/*smc03784*	CpaM-like polysaccharide deacetylase		CpaM (39)	Atu2773 (59)	Blr0435 (38)	NGR_c31780 (74)
pSymA *flp-2*						
C770_GR4pC0512/*sma1580**	CpaI-like putative pili related protein		CpaI (32)	Atu0226 (31)	Blr1444 (37)	NGR_b03710 (59)
C770_GR4pC0513/*sma1579**	Putative pili related protein				Blr3498 (24)	NGR_b03660 (74)
C770_GR4pC0514/*sma1578** (*cpaA2*)	Putative prepilin peptidase	TadV (30)	CpaA (38)	CtpB (36)	TadV (43)	NGR_b03670 (71)
C770_GR4pC0515/*sma1576** (*cpaB2*)	Component of the outer membrane secretin complex		CpaB (34)	CtpC (39)	Bll1440 (40)	NGR_b03680 (78)
C770_GR4pC0516/*sma1573* (*cpaE2*)	Putative docking protein of the secretion system		CpaE (43)	CtpF (40)	TadZ (40)	NGR_b03690 (76)
C770_GR4pC0517/*sma1572*	CpaJ-like pseudopilin protein		CpaJ (41)			NGR_b03700 (75)
C770_GR4pC0518/*sma1570* (*pilA2*)	Flp pilin subunit	Flp-1 (34)	PilA (53)	CtpA (55)	Flp-1 (62)	NGR_b03720 (69)
C770_GR4pC0519/*sma1568** (*cpaF2*)	Pilus assembly ATPase	TadA (48)	CpaF (73)	CtpG (69)	TadA (79)	NGR_b03730 (87)
C770_GR4pC0520/*sma1564*	CpaG-like putative inner membrane platform protein	TadB (28)	CpaG (43)	CtpH (41)	TadB Locus 1 (46)	NGR_b03740 (71)
C770_GR4pC0521/*sma1562*	CpaH-like putative inner membrane platform protein	TadC (20)	CpaH (43)	CtpI (49)	TadC Locus 1 (52)	NGR_b03750 (84)
pSymA Locus 3						
C770_GR4pC1351/*sma0163* (*pilQ2*)	RcpA-like putative component of the outer membrane secretin complex	RcpA (28)	CpaC (31)	CtpD (31)	CpaC (40)	NGR_b10860 (40)
C770_GR4pC1350/*sma0164*	Hypothetical lipoprotein				Blr3501 (33)	NGR_b10850 (29)
C770_GR4pC1349/*sma0166*	CpaO/TadD-like TPR containing protein			Atu0215 (31% in 70 aa middle stretch)	TadD Locus 2 (44)	NGR_b10740 (36)

* Sequence identity of 98.4-99.8% at the amino acid level between GR4 and Rm1021 gene products otherwise 100% identical. ‡ BRC ID (https://www.bv-brc.org/).

The *flp-2* cluster located on the pSymA megaplasmid lacks IS elements and homologues to four genes found in the chromosomal *flp-1* cluster (namely *smc04118*, *cpaC1*, *cpaD1* and *smc02824*). In addition, the 10 genes found on the *flp-2* cluster exhibit a different organization compared to the *flp-1* cluster (Figure 1b). Eight of the ten genes in the *flp-2* cluster are organized into two operons [56]. One of them (*pilA2-cpaF2-sma1564-sma1562*) comprises paralogous genes of the *flp-1* cluster encoding a Flp pilin, a pilus assembly ATPase and the two platform proteins of the pilus apparatus, whereas the second operon (*cpaA2-cpaB2-cpaE2-sma1572*) includes paralogous genes of the *flp-1* cluster encoding a prepilin peptidase, a secretin-associated protein, a docking protein for the secretion system, and a pseudopilin. Upstream of *cpaA2*, two other genes with putative roles in pilus biogenesis

could be identified: *sma1580* encoding a CpaI homologue, and *sma1579* coding for a membrane-associated protein with an N-terminal Tad_N domain found in a family of putative Flp pilus-assembly proteins. No genes homologous to *rcpA/cpaC/ctpD* coding for the outer membrane secretin were found associated to *flp-2*, suggesting that this cluster codes for an incomplete secretion system (Figure 2b). Interestingly, outside of the *flp-2* cluster on the pSymA, a locus (Locus 3) of three genes (*pilQ2-sma0164-sma0166*) could be identified, which contains a homolog of *cpaC* and a gene coding for a protein with characteristic features of T4P pilotins (Figure 1b, Figure 2c, Table 1).
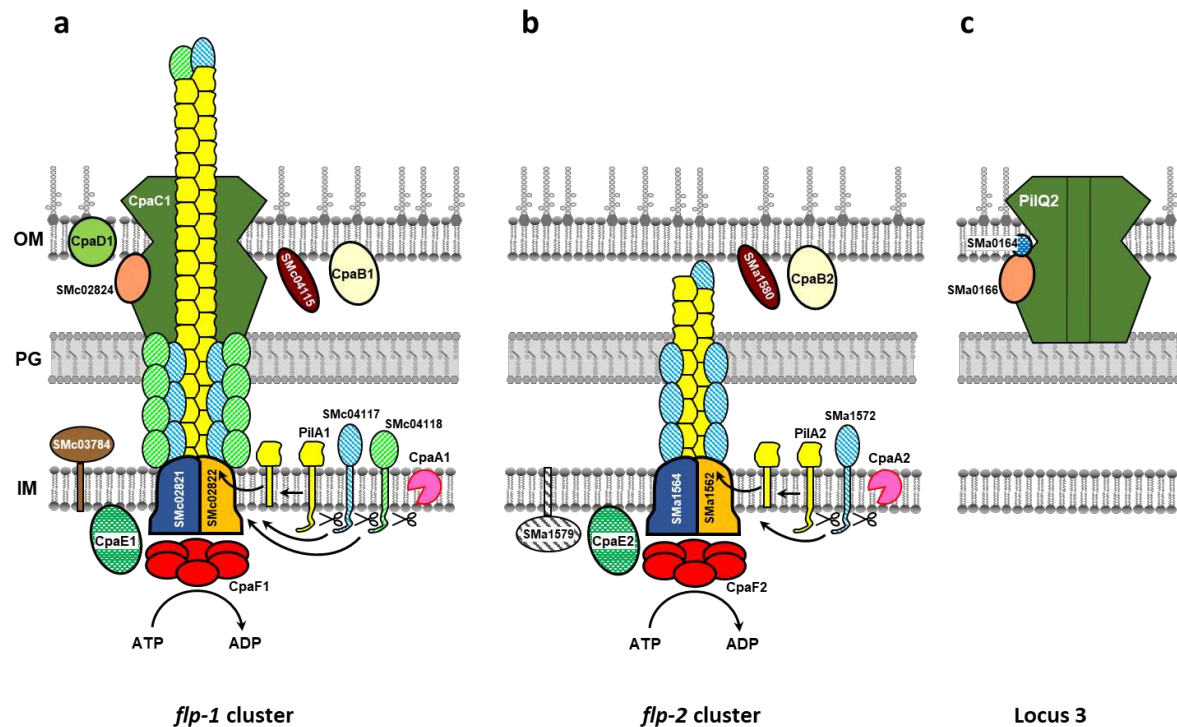
Figure 2. Predictive protein composition and structure of the secretion systems encoded by *S. meliloti tad/cpa* genes of the *flp-1* cluster, *flp-2* cluster and Locus 3. See text for details.

The *pilQ2* gene (name denoting its homology to the PilQ secretin of T4aP) of Locus 3 codes for a 466 amino acid (aa) protein with a signal peptide sequence and a secretin-like domain (Figure S2). This protein shows 31% identity with both *C. vibrioides* CpaC and *A. fabrum* CtpD, and 30% identity with its chromosomal paralogue CpaC1 (Table 1, Figure S2). Downstream of *pilQ2* and forming part of the same operon [56] is *sma0164*, which codes for a hypothetical 98 aa protein that exhibits significant similarities with proteins encoded by *NGR_b10850* and *blr3501*, which are genes associated to T4cP loci in *Sinorhizobium fredii* NGR234 and *B. diazoefficiens*, respectively (Figure 1b, Figure S3). The three proteins contain a prokaryotic membrane lipoprotein lipid attachment profile as identified by InterPro (Figure S3). The profile comprises a precursor signal peptide containing the lipobox motif LXXC that is processed by signal peptidase 2, which cuts upstream of the conserved cysteine residue to which a diacylglycerol is attached [59,60]. The third gene of Locus 3 is *sma0166* encoding a conserved hypothetical protein of 176 aas. Although this protein does not exhibit significant homology with CpaO from *C. vibrioides* or TadD from *A. actinomycetemcomitans*, all three of these proteins contain a TPR motif (Figure S4). This motif, which is involved in protein-protein interactions and in the assembly of multiprotein complexes [61], is also found in the pilotins TadD and PilF of *Pseudomonas aeruginosa* [40]. Moreover, and although PROSITE does not identify a prokaryotic membrane lipoprotein profile associated to SMa0166, a lipobox motif is found in the N-terminal region of the protein (Figure S4). The presence in Locus 3 of genes putatively coding for a CpaC homologue and a putative pilotin opens the possibility that this locus complements the *flp-2* cluster to function as a complete Flp pilus biogenesis and secretion system.

S. meliloti T4cP-related genes identified in the bioinformatic analyses were compared to T4cP-related genes reported in bacteria belonging to *Rhizobiaceae* namely the *ctp* genes of *A. fabrum* C58 [38], genes of *S. fredii* NGR234 [51], and the *tad/cpa* genes of *B. diazoefficiens* USDA 110 [50] (see Figure 1, Table 1). As expected, the highest similarity both in gene organization as well as in sequence is shared between gene clusters from the same genera, *Sinorhizobium*. In this manner, the *flp-1* gene cluster of *S. meliloti* shares the highest similarity with the chromosomal Locus 1 of *S. fredii* NGR324 and the *flp-2* cluster with Locus 2 located on the pNGR234b replicon of *S. fredii* NGR234. The cluster of genes in Locus 3 of *S. meliloti* GR4 and Sm1021 shares the highest similarity with the *cpaC-blr3501-tadD* genes of Locus 2 of *B. diazoefficiens*. The operon encoding the additional Flp pilin found in the chromosome outside of the *flp-1* cluster is the most similar to that found upstream of Locus 1 of *S. fredii* NGR234 and in the linear chromosome of *A. fabrum* C58. In general, the sequence identity between the gene products of the *tad/cpa* gene clusters is higher with orthologues in other bacteria than with paralogues of *S. meliloti* GR4 (Table 1, Table S1) suggesting their origin not to be due to gene duplication events within the same strain.

2.2. Both flp-1 and flp-2 clusters contribute to T4cP production in S. meliloti GR4

In strain Rm1021, formation of Flp pili has been associated to the *flp-1* cluster since pilus-like filaments were mostly absent in cells with a *pilA1* deletion [53]. However, the rare observation of pilus-like structures in a small percentage of *pilA1* mutant cells led the authors to suggest the possibility of pili formation associated either with the expression of the *flp-2* cluster or to the incorporation of the Flp pilin encoded by *smc02446*. To confirm whether both *flp-1* and *flp-2* clusters are responsible for the formation of Flp pili in *S. meliloti* GR4, single and double partial cluster mutants were constructed. Although this approach has the drawback of difficulting complementation experiments, it has the advantage of reducing the probability of obtaining unconclusive results due to the possible complementary effect of paralogous genes. In mutant GRflp1, the genes *pilA1*, *cpaA1*, *cpaB1*, *cpaC1*, *cpaD1*, *cpaE1*, and *cpaF1* were deleted, whereas mutant GRflp2 harbors a deleted version of the *flp-2* cluster in which the *pilA2*, *cpaF2*, *sma1564* and *sma1562* genes were removed (Figure S5). In addition, the GRflp1flp2 double mutant was generated with deleted forms of both the *flp-1* and *flp-2* clusters. The wild-type and *flp* single and double mutant strains were examined for the presence of Flp pili by transmission electron microscopy (TEM). For this purpose, cells grown on solid media were used. Two different cell-surface appendages were observed in the wild-type *S. meliloti* GR4: flagella corresponding to the thicker and more curved filaments, and less abundant, long, thinner and straighter pili-like structures that were often found forming bundles and connecting bacterial cells (Figure 3a,b, Figure S6a,b). The characteristics showed by the the thinner filaments resembled those described for Flp pili of different bacteria, including *S. meliloti* Rm1021 [38,45,53]. However, neither in the single *flp* mutants nor in the double mutant could pili-like structures be observed, and only flagella were evident as cell-surface appendages (Figure S6). In order to facilitate the detection of pili structures, *flp* mutants were created in the flagellaless background offered by the *flaAflaB* mutant. Due to the lack of the major flagellin FlaA, the *flaAflaB* mutant cannot produce normal functional flagella and instead short, straight filamentous structures resulting from mutant broken filaments can be observed [10]. Micrographs of the different flagellaless strains revealed that, in addition to the short broken flagellar filaments, pili-like structures were also evident in the *flaAflaB* mutant (Figure 3c,d) and in its *flp* simple derivative mutants (Figure 3e,f,g,h) but not in the flagellaless *Δflp-1Δflp-2* double mutant (Figure 3i,j). This suggests that both *flp* clusters function to make pili-like structures.
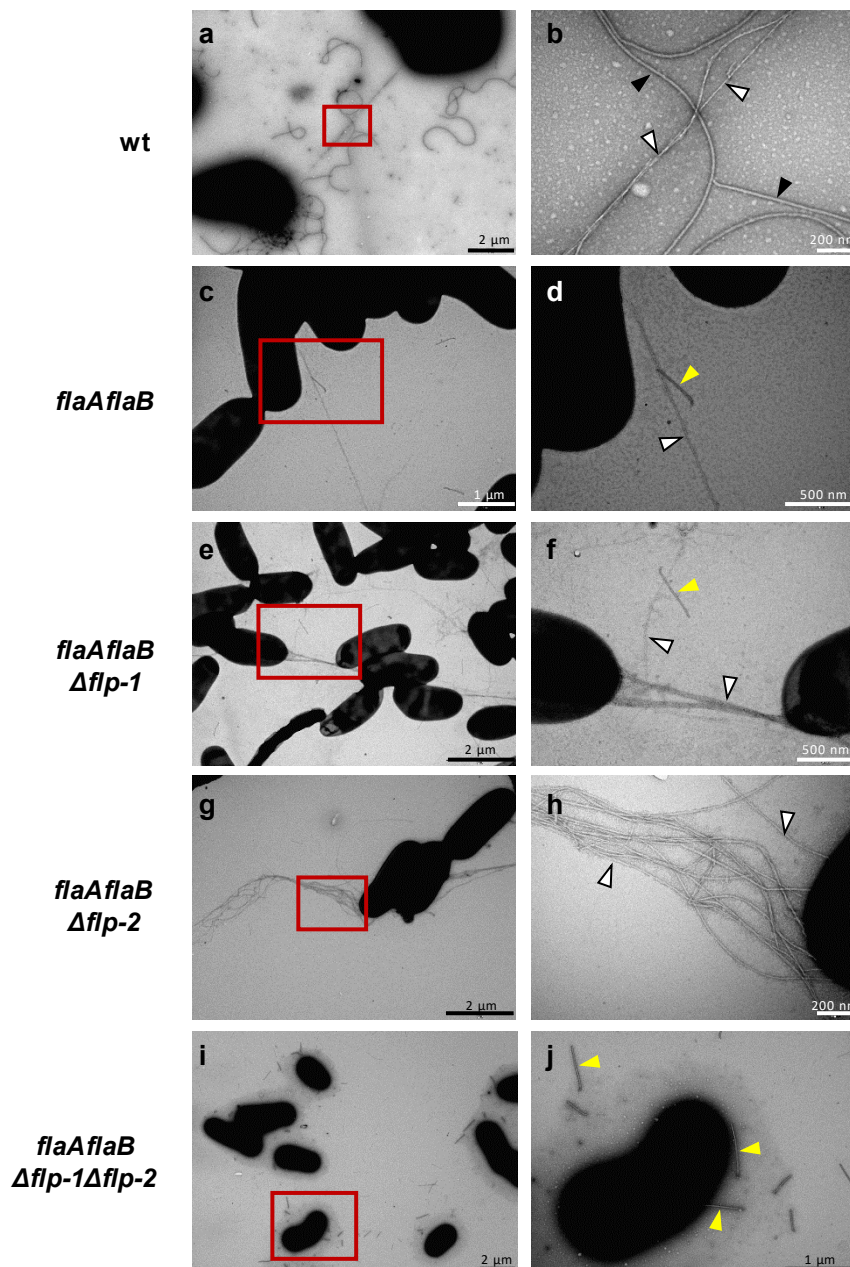
Figure 3. Transmission electron microscopy of *S. meliloti* strains. Micrographs were obtained from cells grown overnight on solid MM (1%) and negatively stained with uranyl acetate (2%). Each right panel is a closer view of the red inlet indicated in the corresponding left panel. Wild-type strain GR4 (**a-b**) and flagellaless strains GR4flaAB (**c-d**), GRflaflp1 (**e-f**), GRflaflp2 (**g-h**), and GRflaflp1flp2 (**i-j**). Black and white arrowheads indicate flagella and Flp pili, respectively. Yellow arrowheads indicate short broken flagellar filaments characteristic of *flaAflaB* mutants.

2.3. Type IVc Pili (T4cP) facilitate surface spreading of S. meliloti GR4

Pili can mediate different types of surface motility [29]. In *C. crescentus*, Tad pili are able to promote twitching- or walking-like movements [62]. To evaluate the effect of T4cP in *S. meliloti* GR4 translocation, wild-type as well as single and double *flp* mutant derivative strains were assessed in different motility assays. Using different media, agar sources and concentrations under the experimental conditions known to promote twitching motility in different bacteria [63], similar limited spreading in the agar/plate interphase was observed for all of the strains (Figure S7). Since no differences were detected between the wild type and the *flp* mutants in this type of assay, it remains unclear whether the limited spreading observed was due to twitching or to other forms of bacterial motility. Nonetheless, it appears that the *flp* clusters are not involved in this trait. In contrast, when

motility was assessed under conditions that promote swarming in strain GR4 [10], some differences were observed between the wild type and *flp* derivative mutants. Of the 18 replicates, the frequency of swarming observed for the parental strain was 100%, while 89%, 61% and 67% frequencies were observed for the deletion mutants *Δflp-1*, *Δflp-2*, and *Δflp-1Δflp-2*, respectively. Pairwise comparison using the Chi square statistic indicated significant difference (P<0.01) between the swarming frequency of the wild-type compared to either *Δflp-2* or *Δflp-1Δflp-2* but not *Δflp-1*. With respect to the magnitude of surface spreading, surface motility was affected in all mutant strains and significantly so in the double mutant *Δflp-1Δflp-2* (Figure 4a,b). These results suggest that the inactivation of the *flp-2* cluster has a stronger effect in surface motility than the inactivation of the *flp-1* cluster and that this effect was cumulative in the double mutant. When swimming motility was tested in BM (0.3%), all three *flp* deletion mutants exhibited a slight but significant decrease in their swimming halo compared to that of the wild-type strain, with both the single mutants and the double mutant being equally affected (Figure 4c,d).
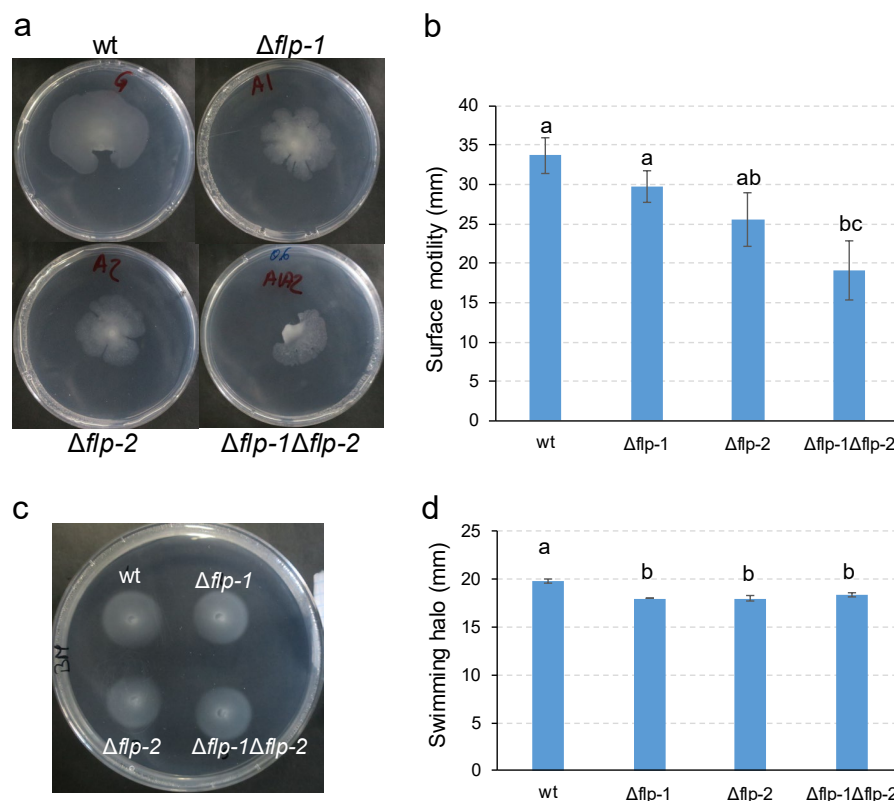
Figure 4. Surface and swimming motilities exhibited by GR4-derivative *flp* deletion mutants. (**a**) Representative pictures and (**b**) graph of the surface motilities exhibited after 48 h of incubation on MM (0.6 % agar). (**c**) Representative picture and (**d**) graph of the swimming motilities in BM (0.3 % agar) after 72 h of incubation. Bars represent standard error of the mean and the different letters indicate significant differences according to an analysis-of-variance (ANOVA) test (P≤0.05).

2.4. The interaction of S. meliloti GR4 with alfalfa is influenced by T4cP

Deletion of the *pilA1* gene in *S. meliloti* strain Rm1021 reduced competitiveness for nodule occupancy when confronted with the wild type, indicating that Flp pili play a role in Rm1021 symbiotic performance [53]. However, to the best of our knowledge, the role of the pSymA-encoded Flp pili in symbiosis has not yet been reported. In addition, *S. meliloti* strains Rm1021 and GR4 present remarkable differences including some symbiotic properties with the latter being more efficient in colonizing alfalfa roots and exhibiting higher competitive ability than Rm1021 [9,55]. In this study, the contribution of chromosomal and pSymA-encoded T4cP in the interaction of GR4 with alfalfa plants was investigated. No differences in bacterial attachment to alfalfa roots were found between the wild-type strain or any of the single *flp* mutants as indicated by the similar number of colony forming units (CFUs) associated to plant roots 2 hours after inoculation (Figure 5). Likewise, the single *flp* deletion mutants colonized plant roots as efficiently as the wild-type after 24, 48 and 72 hours (Figure 5). In contrast, we found that the double Δ*flp-1*Δ*flp-2* mutant shows increased adhesion to root surfaces 2 hours post-inoculation compared to the wild-type and the single *flp* mutants (Figure 5). Remarkably, the increased capacity to attach to root surfaces exhibited by the double mutant does not result in increased bacterial colonization of roots. Indeed, 72 h after inoculation, the number of Δ*flp-1*Δ*flp-2* CFUs associated to roots was lower than in the wild type, although this difference was not significant. These results indicate that the presence of either of the two Flp pili produced by *S. meliloti* reduces bacterial attachment to alfalfa roots but this effect does not preclude efficient colonization of the plant host.
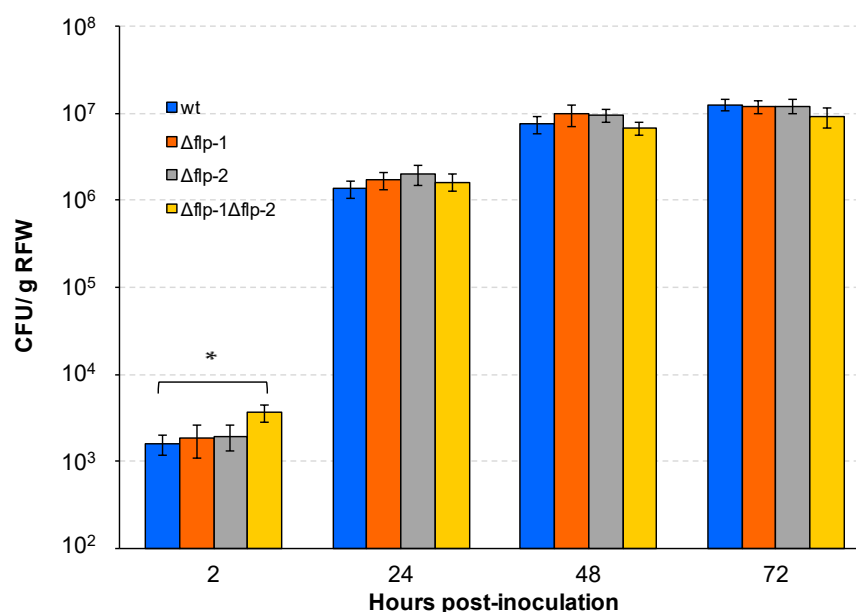

Figure 5. Bacterial attachment to and colonization of alfalfa roots by *flp* deletion mutants of *S. meliloti*. Colony forming units (CFU) recovered from alfalfa roots were determined 2 hours after inoculation to determine bacterial adhesion, and 24, 48 and 72 h post-inoculation to assess the colonization ability of each bacterial strain. Data are expressed per gram of root fresh weight (RFW). Error bars indicate the standard error of the mean. The asterisk indicates significant difference according to an ANOVA test (P≤0.05).

Next, to determine whether the *flp* clusters had an effect on the symbiotic interaction with alfalfa plants, infectivity and competitive abilities of the single and double *flp* mutants were assayed (Figure 6). All three mutants were able to induce the formation of nitrogen-fixing nodules and no differences in the nodule formation efficiency were detected in the single *flp* mutants compared with the wild-type (Figure 6a). However, the number of nodules induced by the double mutant was slightly but significantly lower than those of the wild type or single *flp* mutants at the end of the experiment (13

and 15 days post-inoculation) (Figure 6a). We also determined the competitive ability for nodule occupancy of the *flp* mutants by inoculating alfalfa plants with bacterial mixtures of the strain to be tested and a marked wild-type strain (*S. meliloti* GR4 (pGUS3)) at a ratio of 1:1. These competition assays showed that the *Δflp-2* mutant showed a significantly lower nodule occupancy than the wild-type strain (Figure 6b). Notably, the reduction in competitiveness was not observed in the double *Δflp-1Δflp-2* mutant (Figure 6b), indicating that the lack of T4cP from cluster *flp-2* reduces the bacterial competitive ability for nodule occupation only when T4cP from the *flp-1* cluster are present. Altogether, these results demonstrate that both *flp-1-* and *flp-2*-dependent pili influence *S. meliloti* symbiotic fitness.
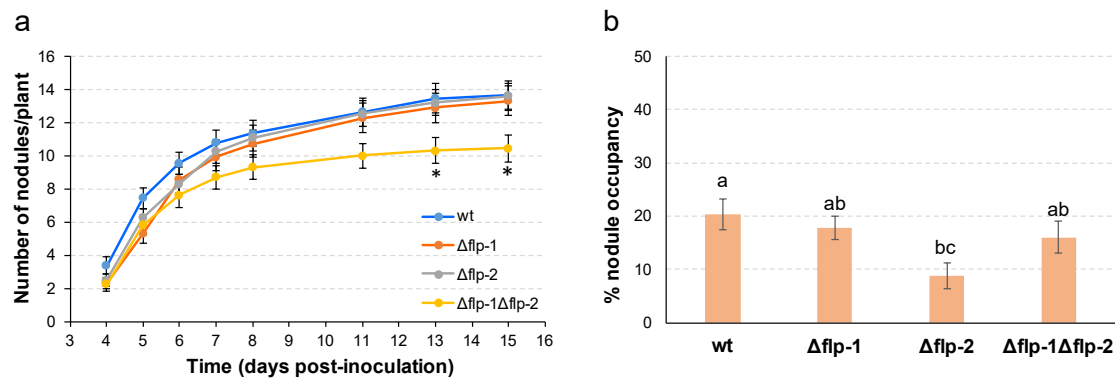
Figure 6. Symbiotic phenotype of GR4-derivative *flp* deletion mutants. (**a**) Nodulation kinetics of alfalfa plants inoculated with *S. meliloti* wild-type GR4, or their derivative single and double *flp* deletion mutants. Data represent the average number of nodules per plant. The bars represent standard errors from 38 replicates in two independent experiments. Asterisks indicate significant differences compared to the wild-type according to an ANOVA test (P≤0.05). (**b**) Competitive nodulation assays. Data represent the percentage of nodules occupied by each rhizobial strain after co-inoculation with the marked strain GR4 (pGUS3) in a mixture ratio of 1:1. Error bars indicate the standard error of the mean obtained from three independent experiments. Different letters indicate significant differences according to an ANOVA test (P≤0.05).

3. Discussion

This work provides insights into T4cP in rhizobia by uncovering the role of the two *flp* clusters present in the highly competitive *S. meliloti* strain GR4. We show that both *flp-1* and *flp-2* are functional in the biogenesis of pili-like structures, and both contribute to the optimal surface translocation exhibited by this rhizobial strain. Our data indicate that, although these *flp* clusters are dispensable for the formation of nitrogen-fixing nodules, they modulate symbiotic characteristics that might confer adaptive advantages such as bacterial attachment to plant roots, nodule formation efficiency and bacterial competitiveness for nodule occupation.

Despite the participation of T4cP in diverse microbial lifestyles [27,29,44], it is striking that to date, only two studies have addressed the role of T4cP genes in two different rhizobial species [50,53]. Most likely, the abundance of *tad/cpa* genes in rhizobial genomes [11,35] together with the subtle phenotypes exhibited by T4cP-related mutants under laboratory conditions, discouraged further investigations on these filaments in the legume symbionts. Our bioinformatic analyses identified up to 29 genes putatively related to T4cP in *S. meliloti*. This number contrasts with the relatively lower number of *tad/cpa* genes (14-16 genes) found in *A. actinomycetemcomitans* and *C. vibrioides* [32,37,57]. Remarkably, the number of loci putatively related to T4cP is even higher in other rhizobia such as *S. fredii* NGR234 (47 genes) and *B. diazoefficiens* USDA 110 (39 genes). The maintenance of such a number of pili-related genes throughout evolution could be an indication of the significant adaptive advantages conferred by pili to rhizobial lifestyles. Another remarkable feature of T4cP-related genes in rhizobia compared to *tad/cpa* genes in *A. actinomycetemcomitans* and *C. vibrioides* is their organization in various clusters. In addition to a chromosomal cluster that appears to be conserved

in phylogenetically distant bacteria, the three rhizobial species analyzed in our study contain other clusters located in either the chromosome (*B. diazoefficiens*) or in megaplasmids (pSymA of *S. meliloti* and pNGR234b of *S. fredii* NGR234). The existence of more than one cluster of *tad/cpa* genes is not unique to rhizobia [35,45,64]. Like in *S. meliloti*, in the bacterial wilt pathogen *Ralstonia solanacearum* two distinct *tad* clusters located in the megaplasmid and chromosome were identified [45]. Characterization of a *tadA2* mutant of this bacterium revealed that the Flp pili associated to the megaplasmid cluster are required for virulence on potato plants [45] whereas no information exists regarding the function of the chromosomal cluster. The opportunistic animal pathogen *Vibrio vulnificus* harbors three *tad* loci and only the triple mutant exhibited decreased virulence in mice, indicating that the *tad* loci work cooperatively in this species during pathogenicity [64].

In *S. meliloti,* the chromosomal *flp-1* cluster carries all of the genes needed for T4cP biogenesis, and the formation of bundle-forming pili was previously associated to this cluster in strain Rm1021 [53]. In contrast, *flp-2* lacks some key genes for the secretion system to be functional. The lack of *cpaK* and *cpaD* homologues should not be an impediment for T4cP biogenesis. Indeed, *A. fabrum* and *Pseudomonas aeruginosa* are capable of assembling Flp pili in the absence of *cpaK* and *cpaD* homologues, respectively [38,65]. However, the lack of genes coding for components of the outer membrane secretin channel (*cpaC* and *cpaO*) could prevent pilus biogenesis associated to the *flp-2* cluster. Interestingly, an additional set of three genes located on pSymA (Locus 3) was identified that could complement genes in *flp-2*. Indeed, TEM analysis of flagellaless mutants carrying single large deletions in either the *flp-1* or *flp-2* clusters revealed the production of filaments while these fimbriae structures were no longer observed in a flagellaless double *flp-1flp-2* mutant. These results indicate that, under our experimental conditions, the two *flp* clusters are functional in the formation of pili. In the study carried out by Zatakia and co-workers (2014)[53], pili-like structures were only rarely observed in the *pilA1* mutant of Rm1021, which the authors explained as the result of T4cP assembly from the *flp-2* cluster and/or the incorporation of the pilin encoded by the orphan *smc02446* gene. The latter is a very likely possibility considering that the two pilin genes in *A. fabrum*, *ctpA* and *pilA*, are functionally interchangeable [38]. The approach used in our study in which deletions of gene clusters were generated in the *flp* regions instead of deleting individual genes, reduces the possibility of inconclusive results due to possible complementation effects of paralogous genes. In our *flaAflaB△flp-1* mutant, in which not only *pilA1* but also *cpaA1, cpaB1, cpaC1, cpaD1, cpaE1* and *cpaF1* were deleted, pili forming bundles connecting cells were clearly observed that cannot be the result of the incorporation of the *smc02446*-encoded pilin. Moreover, pili-like structures could not be detected in *flaAflaB△flp-1△flp-2* indicating that the filaments observed in *flaAflaB△flp-1* are due to a fully functional *flp-2* cluster, possibly with the implication of Locus 3 which contains all three genes missing in *flp-2*. However, experiments are still needed to demonstrate that Locus 3 is essential for pili biogenesis associated to the *flp-2* cluster.

The splitting of genes required for the assembly of T4cP in distinct genetic clusters is not usual [28] but at least one example has been reported in the literature. In the bacterial predator *Myxococcus xanthus*, the assembly of the Tad-like Kil system involved in contact-dependent prey killing is the result of the expression of two clusters that carry complementary sets of genes [44]. In addition, our bioinformatic analyses revealed that in *S. fredii*, Locus 2 on pNGR234b shows high similarity both in gene organization and sequence with *S. meliloti flp*-2 and, like the latter, it also lacks genes coding for the secretin complex. Homologs to *S. meliloti* Locus 3 genes can be identified in a different region in pNGR234b (*NGR_b10860*, *NGR_b10850* and *NGR_b10740* in Locus 3), albeit exhibiting a different gene organization and clustered together with additional T4cP-related genes. Clearly, further investigations are needed in order to elucidate if distinct co-existing *tad/flp* clusters in rhizobia play different or specific roles or if they have complementary functions.

In this work, pili-like structures were more easily detectable in the flagellaless strains containing one or the two *flp* clusters than in the wild type strain GR4 (Figure 3). A simple explanation could be that the abundant flagellar filaments present in the wild-type strain are hampering the observation of the thinner and scarcer pili-like structures. However, the possibility that the lack of flagellar filaments has an impact on T4cP gene expression in *S. meliloti* should not be discarded and deserves

further investigation. In bacteria in which T4cP have been studied the most, expression of the pilus associated genes and activity of the filament are controlled by complex transcriptional and posttranslational regulatory mechanisms [29,35]. In *P. aeruginosa*, a feedback regulation between pili and flagellar components occurs through a two-component regulatory system [66]. Moreover, *C. crescentus* flagellar mutants are significantly deficient in pili biogenesis and it was suggested that different stages of the flagellum assembly act as checkpoints for the regulation of T4cP associated gene expression [67]. Another open question that was not addressed in this study is whether the two *flp* clusters in *S. meliloti* are expressed under the same conditions. The presence of an accessory chemotaxis system next to the *flp-2* cluster in pSymA is intriguing. This chemotaxis system belongs to the alternative cellular function (ACF) and most likely does not control flagella [11]. It would be worth investigating whether this chemotaxis system controls the activity of T4cP in *S. meliloti* in an analogous way to how the Pil-Chp pathway controls T4aP in other bacteria [68].

Tad pili are able to promote twitching- or walking-like movements in *C. crescentus* [62]. Surface motility assays performed with our *S. meliloti flp* deletion mutants indicate that the *flp* clusters contribute cooperatively to the optimal surface motility exhibited by strain GR4 with the *flp-2* cluster having a stronger effect than *flp-1*. Under the experimental conditions used in our study, surface motility in GR4 is totally dependent on flagellar action [10]. At present, we can only speculate about how *flp-1* and *flp-2* affect swarming motility in GR4. Our data indicate that the double *flp-1flp-2* mutant exhibits greater attachment to alfalfa roots compared to the wild type (Figure 5). An increased adhesion to surfaces facilitated by the absence of pili could hamper proper bacterial translocation. On the other hand, pili together with flagella participate in surface sensing in bacteria [69] and specifically Tad pili act as surface contact sensors for *C. crescentus* [30,62,70]. An attractive possibility awaiting investigation is that pilus-based mechanosensation in *S. meliloti* triggers a signal transduction cascade that promotes swarming and other physiological adaptations to thrive on surfaces.

Information about the role of T4cP in the establishment of symbiosis with legumes is very scarce. Results obtained in this study indicate that T4cP impact the symbiotic fitness of *S. meliloti* by affecting adhesion to plant roots, nodule formation efficiency and competitiveness. The role of rhizobial T4cP in favoring adhesion to plant roots has been previously proposed in two studies [50,53]. In *B. diazoefficiens* USDA 110, inactivation of *tadG* or the cluster *tadGEF* (Locus 3 of *B. diazoefficiens* USDA 110 in Figure 1b) impaired adhesion to soybean roots and caused delayed root infection [50]. However, the connection between the symbiotic phenotype of *tadGEF* mutants and pili formation in *B. diazoefficiens* USDA 110 was not directly examined. In contrast to *B. diazoefficiens* and *S. fredii* NGR234, no *tadG* homologue could be identified in the genome of *S. meliloti*. On the other hand, the reduced competitive ability for nodule occupation exhibited by a *S. meliloti pilA1* mutant was suggested to be due to a lower bacterial attachment to plant roots, although this possibility was not experimentally tested [53]. Results obtained in our study do not support a role for *S. meliloti* T4cP in promoting adhesion to root surfaces. As already discussed, the double *flp-1flp-2* mutant, which lacks pili-like structures, exhibits greater attachment to plant roots compared to the wild-type and single *flp* mutant strains (Figure 5). These observations demonstrate that T4cP are not required for attachment of *S. meliloti* cells to alfalfa roots, and suggest that the presence of T4cP hamper attachment to the root surface mediated by other cell surface structures, perhaps flagella, exopolysaccharides and/or lipopolysaccharide [4].

Our data also demonstrate that the increased binding to root surfaces shown by the double *flp* cluster mutant does not significantly affect the biofilm formed on plant roots 24, 48 or 72 hours after inoculation, indicating that, under our experimental conditions, *S. meliloti* T4cP are not essential for plant root colonization during the early stages of the interaction. Likewise, in *A. fabrum* no differences were detected between the 48 h biofilm formed on *Arabidopsis thaliana* roots by the wild-type strain and a *ctpA* derivative mutant [38]. Nevertheless, our *S. meliloti* double *flp* mutant showed decreased nodule formation efficiency indicated by the significantly lower number of nodules induced by this strain compared to the wild type or single *flp* mutants. At present, the reasons for the lower nodulation performance of the double *flp* mutant are unknown. Perhaps the increased attachment to

the root surface shown by the mutant together with the lower ability to move across surfaces reduces the probability of rhizobial cells to find potential infection sites. Another, non-excluding possibility is that T4cP, directly or indirectly, contribute to defend *S. meliloti* cells against plant defense responses with a role similar to the stealth hiding role proposed for the Tad pili in *V. vulnificus* [64].

Finally, our data show that deletion of *flp-1* in GR4 does not affect its competitive ability for nodule occupation. This result contrasts with the lower competitiveness exhibited by a *pilA1* deletion mutant compared with its corresponding wild- type strain Rm1021 [53]. Differences between GR4 and Rm1021 and/or the type of mutation used to analyse the role of T4cP associated to *flp-1*, could explain the contrasting results obtained in the two studies. Interestingly, although the lack of *flp-1* has no influence on GR4 competitiveness, the presence of this cluster in a *flp-2* deletion mutant reduces its ability to compete for nodule occupation. This is based on the lower nodule occupancy exhibited by the single *flp-2* mutant that is recovered when *flp-1* is deleted. A possible explanation for this result is that in the absence of *flp-2* pili, interbacterial attachment mediated by Flp-1 pili is increased, which could hamper dissemination to other infection sites. This seems not to be crucial in single inoculation experiments as shown by similar nodulation kinetics of the *flp-2* mutant and the wild-type strain, but confers a disadvantage when competing with another bacterium.

In summary, this study increases our knowledge on T4cP in *S. meliloti* and their role in the interaction with its plant host, and at the same time, highlights the complexity of their study. New questions have arisen and investigations aimed to answer them might help us to better understand how extracellular filament appendages contribute to the symbiotic fitness of rhizobia.

4. Materials and Methods

4.1. Bacterial strains, plasmids and growth conditions

Bacterial strains and plasmids used in this work are listed in Table S2. *Escherichia coli* cultures were routinely grown in LB medium [71] at 37°C. *S. meliloti* strains were grown in either complex tryptone yeast (TY) medium [72] or in Robertsen minimal medium (MM) [73] at 28°C. When required, antibiotics were added to final concentrations (μg mL^{-1}) of: 50 kanamycin and 25 hygromycin for *E. coli*; 200 kanamycin and 75 hygromycin for *S. meliloti*. All reagents were obtained from Sigma-Aldrich (Steinheim, Germany), unless otherwise specified.

4.2. In silico analyses

In order to identify and compare *tad/cpa/ctp* genes from *S. meliloti* GR4, *A. actinomycetemcomitans* CU1000N, *C. vibrioides* NA1000, *A. fabrum* C58, *S. fredii* NGR234 and *B. diazoefficiens* USDA110, genome sequences were retrieved from the NCBI database (https://www.ncbi.nlm.nih.gov/datasets/genome/). Comparisons of these genomes were performed in the Rapid Annotations using Subsystems Technology (RAST) server version 2.0 [74]. Further gene identification was performed using resources at KEGG (https://www.genome.jp/kegg/ , [75]) and BV-BRC (https://www.bv-brc.org/ , [76]. Sequence comparisons of individual gene products were performed with blastp (https://blast.ncbi.nlm.nih.gov/Blast.cgi) and Clustal MUSCLE sequence alignment at https://www.ebi.ac.uk/Tools/msa/muscle/. Protein domains within individual gene products were examined using InterPro (https://www.ebi.ac.uk/interpro/ , [77]).

4.3. Construction of S. meliloti mutant strains

flp-1 and *flp-2* mutants were obtained by allelic exchange of each *flp* cluster with markerless deleted versions obtained *in vitro* by overlap extension PCR using primers delpilA1.1 to delpilA1.4 and delpilA2.1 to delpilA2.4 (Table S3) and Phusion high-fidelity DNA polymerase. The resulting amplicons corresponding to deleted versions of *flp-1* and *flp-2* were first cloned into pCR-XL-TOPO and confirmed by DNA sequencing and then, subcloned into pK18*mobsacB* as *Bam*HI or *Hin*dIII fragments to give pK18-Δflp1 and pK18-Δflp2, respectively. Each one of these constructions was introduced into *S. meliloti* GR4 by conjugation using S17-1 as the donor strain [78] and the allelic exchange was selected as previously described [79] to obtain the single GRflp1 and GRflp2 mutants.

The double GRflp1flp2 mutant was generated by selecting the allelic exchange of the *flp-2* cluster with the corresponding deleted version in the single GRflp1 mutant. To obtain flagellaless *flp* mutants, plasmid pK18flaAB::Hyg was introduced into single and double *flp* mutants and replacement of wild type flagellin genes with the mutated version was selected on plates containing hygromycin. All mutants were checked by Southern hybridization with specific probes.

4.4. Transmission electron microscopy (TEM)

Cells for TEM observations were obtained using the same procedures as that described in Calatrava-Morales et al. (2017) [80] from the edge of colonies grown on solid MM (1% agar). In brief, carbon-coated Formvar grids were placed for 5 min on top of a drop of water (sterile MilliQ) previously applied to the colony border. The grids were then washed twice in water for 1 min and stained with 2% (wt/vol) uranyl acetate for 3 min. Grids were allowed to air dry for at least 1 h and visualized using a JEOL JEM-1011 transmission electron microscope with a 100-kV beam at the Microscopy Service of the Estación Experimental del Zaidín (Granada, Spain). Images were captured with an Olympus SIS Megaview III CCD camera for TEM.

4.5. Motility assays

To determine swimming motility, *S. meliloti* strains were grown in liquid TY medium at 28 ºC until they reached an optical density (OD_{600nm}) of approximately 0.5. Aliquots of 3 µL of each culture were placed onto plates containing Bromfield medium (BM) (0.04% tryptone, 0.01% yeast extract, 0.01% $CaCl_2 \times 2H_2O$, 0.3% Bacto Agar, Difco BM). After incubation at 28°C for 72 hours, the dispersion halo of each colony was measured.

Swarming motility assays were performed as described by López-Lara et al. (2018) [81]. Briefly, cultures of the *S. meliloti* strains in liquid TY medium were grown overnight to an OD_{600} greater than 1. Subsequently, each culture was washed twice with liquid MM and after the last wash, the pellet was resuspended in 80 µL of liquid MM. 2 µL aliquots of the suspension were inoculated and allowed to dry for 10 minutes onto the surface of MM plates (0.6% noble agar, Difco BM), which were previously dried for 15 min. The plates were incubated at 28°C for 48 hours. To quantify motility, the length of each of the sides of the extended colony was measured in millimeters. Colonies which had extended 7 mm or further were considered positive in swarming.

Twitching motility was assayed according to the protocol described by Turnbull and Whitchurch et al. (2014) [63] with small modifications. Plates containing 10 ml of either TY (1% Bacteriologic Agar), MM (1.3% Agar, Grade A Difco), MM (1% Agar, Grade A Difco) and MM (1% Agar, Noble) were prepared and dried according to the protocol. Strains were stab inoculated with a toothpick to the bottom of the plate and incubated for 2-4 days at 28 °C in a humidified chamber.

4.6. Plant assays

Alfalfa (*Medicago sativa* L. 'Victoria') plants were surface sterilized, germinated, and grown in hydroponic cultures under axenic conditions in glass tubes containing nitrogen-free nutrient solution, as previously described [82].

To test the degree of infectivity of each strain, 9-day-old plants (18-20 replicates, one plant per tube) were inoculated with 1 ml of a rhizobial suspension containing 5×10^6 cells. Prior to inoculation, bacteria were grown to the exponential phase (OD_{600} = 0.5 to 0.6) in TY broth and diluted 100-fold in sterile water. Four days after inoculation, the number of nodules per plant was recorded over two weeks.

To examine competitive ability, 12 individual plants grown as described for the infectivity test were inoculated with 1 ml of a bacterial suspension prepared as already described, containing mixtures at a ratio of 1:1 of the *S. meliloti* strain to be tested and GR4 marked with the pGUS3 plasmid [83]. Roots were collected 15 days after inoculation, briefly washed with water, and incubated overnight in the dark at 37°C in 1 mM 5-bromo-4-chloro-3-indolyl-b-D-glucuronide (Apollo Scientific) in 50 mM sodium phosphate buffer (pH 7.5) with 1% SDS. Those nodules occupied by the

strain harboring the pGUS3 plasmid stained blue; thus, nodule occupancy could be determined by counting blue and white nodules produced by each bacterial mixture in three independent experiments.

Colonization assays were performed as Calatrava-Morales et al. (2017) [80]. Briefly, 1 week old alfalfa plants (5 plants/tube) were inoculated with 1 ml rhizobial suspension as described above. At different times, 15 roots from each treatment were collected and washed three times with sterile distilled water, and pools of roots from 5 plants introduced onto an Eppendorf tube containing sterile Tris-EDTA buffer (10 mM Tris-HCl [pH 7.5] and 1 mM EDTA). Tubes were sonicated (2x for 1 min each) in a Selecta Ultrasons Sonicator bath. Released rhizobia were quantified by counting colony forming units (CFU) of serial dilutions, and data were plotted as CFU per gram of root fresh weight (RFW).

Supplementary Materials: The following supporting information can be downloaded at the website of this paper posted on Preprints.org. Figure S1: Multiple sequence alignment by MUSCLE of Flp prepilins; Figure S2: Multiple sequence alignment by MUSCLE of PilQ2-like gene products; Figure S3: Multiple sequence alignment by MUSCLE of SMa0164 with homologous proteins of *S. fredii* NGR234 (Sf) and *B. diazoefficiens* (Bd); Figure S4: Multiple sequence alignment by MUSCLE of SMa0166 with TadD-like gene products; Figure S5: Genomic regions corresponding to the *flp-1* and *flp-2* clusters of *S. meliloti* GR4 and their corresponding unmarked in-frame deleted versions obtained in this study; Figure S6: Transmission electron microscope (TEM) images of flagella-plus single and double *flp* deletion mutants; Figure S7: Twitching motility assay of duplicate stab inoculations of the different strains on different media with different agar concentrations and types; Table S1: Percent sequence identities (in parenthesis) among *S. meliloti* T4cP paralogues; Table S2: Strains and plasmids used in this study; Table S3: List of primers used in this study.

Author Contributions: Conceptualization, P.v.D., and M.J.S.; formal analysis, C.C.-H., V.C., L.M.B-R., and P.v.D.; investigation, C.C.-H., V.C., and L.M.B-R., and M.J.S.; writing—original draft preparation, C.C.-H., and P.v.D.; writing—review and editing, C.C.-H., V.C., L.M.B-R.; P.v.D., and M.J.S.; visualization, C.C.-H., P.v.D., and M.J.S.; supervision, M.J.S.; funding acquisition, M.J.S. All authors have read and agreed to the published version of the manuscript.

Data Availability Statement: Not applicable.

Conflicts of Interest: The authors declare no conflict of interest. The funders had no role in the design of the study; in the collection, analyses, or interpretation of data; in the writing of the manuscript; or in the decision to publish the results.

References

1. Poole, P.; Ramachandran, V.; Terpolilli, J. Rhizobia: from saprophytes to endosymbionts. *Nat Rev Microbiol* **2018**, *16*, 291-303, DOI: 10.1038/nrmicro.2017.171.
2. Oldroyd, G.E.; Murray, J.D.; Poole, P.S.; Downie, J.A. The rules of engagement in the legume-rhizobial symbiosis. *Annu Rev Genet* **2011**, *45*, 119-144, DOI: 10.1146/annurev-genet-110410-132549.
3. Cangioli, L.; Vaccaro, F.; Fini, M.; Mengoni, A.; Fagorzi, C. Scent of a Symbiont: The Personalized Genetic Relationships of Rhizobium-Plant Interaction. *Int J Mol Sci* **2022**, *23*, 3358, DOI: 10.3390/ijms23063358.
4. Wheatley, R.M.; Poole, P.S. Mechanisms of bacterial attachment to roots. *FEMS Microbiol Rev* **2018**, *42*, 448-461, DOI: 10.1093/femsre/fuy014.
5. Knights, H.E.; Jorrin, B.; Haskett, T.L.; Poole, P.S. Deciphering bacterial mechanisms of root colonization. *Environ Microbiol Rep* **2021**, *13*, 428-444, DOI: 10.1111/1758-2229.12934.
6. Ames, P.; Bergman, K. Competitive advantage provided by bacterial motility in the formation of nodules by *Rhizobium meliloti*. *J Bacteriol* **1981**, *148*, 728-908, DOI: 10.1128/jb.148.2.728-729.1981.
7. Soby, S.; Bergman, K. Motility and Chemotaxis of *Rhizobium meliloti* in Soil. *Appl Environ Microbiol* **1983**, *46*, 995-998, DOI: 10.1128/aem.46.5.995-998.1983.
8. Caetano-Anollés, G.; Wrobel-Boerner, E.; Bauer, W.D. Growth and Movement of Spot Inoculated *Rhizobium meliloti* on the Root Surface of Alfalfa. *Plant Physiol* **1992**, *98*, 1181-1189, DOI: 10.1104/pp.98.3.1181.

9. Amaya-Gómez, C.V.; Hirsch, A.M.; Soto, M.J. Biofilm formation assessment in *Sinorhizobium meliloti* reveals interlinked control with surface motility. *BMC Microbiol* **2015**, *15*, 58, DOI: 10.1186/s12866-015-0390-z.

10. Bernabéu-Roda, L.; Calatrava-Morales, N.; Cuéllar, V.; Soto, M. Characterization of surface motility in *Sinorhizobium meliloti*: regulation and role in symbiosis. *Symbiosis* **2015**, 1-12, DOI: 10.1007/s13199-015-0340-4.

11. Aroney, S.T.N.; Poole, P.S.; Sanchez-Canizares, C. Rhizobial Chemotaxis and Motility Systems at Work in the Soil. *Front Plant Sci* **2021**, *12*, 725338, DOI: 10.3389/fpls.2021.725338.

12. Soto, M.J.; Fernández-Pascual, M.; Sanjuán, J.; Olivares, J. A *fadD* mutant of *Sinorhizobium meliloti* shows multicellular swarming migration and is impaired in nodulation efficiency on alfalfa roots. *Mol. Microbiol* **2002**, *43*, 371-382, DOI: 10.1046/j.1365-2958.2002.02749.x.

13. Nogales, J.; Bernabéu-Roda, L.; Cuéllar, V.; Soto, M.J. ExpR is not required for swarming but promotes sliding in *Sinorhizobium meliloti*. *J Bacteriol* **2012**, *194*, 2027-2035, DOI: 10.1128/JB.06524-11.

14. Dilanji, G.E.; Teplitski, M.; Hagen, S.J. Entropy-driven motility of *Sinorhizobium meliloti* on a semi-solid surface. *Proc Biol Sci* **2014**, *281*, 20132575, DOI: 10.1098/rspb.2013.2575.

15. Ji, Y.Y.; Zhang, B.; Zhang, P.; Chen, L.C.; Si, Y.W.; Wan, X.Y.; Li, C.; Wang, R.H.; Tian, Y.; Zhang, Z., *et al.* Rhizobial migration toward roots mediated by FadL-ExoFQP modulation of extracellular long-chain AHLs. *ISME J* **2023**, *17*, 417-431, DOI: 10.1038/s41396-023-01357-5.

16. Kearns, D.B. A field guide to bacterial swarming motility. *Nat Rev Microbiol* **2010**, *8*, 634-644, DOI: 10.1038/nrmicro2405.

17. Mattingly, A.E.; Weaver, A.A.; Dimkovikj, A.; Shrout, J.D. Assessing Travel Conditions: Environmental and Host Influences On Bacterial Surface Motility. *J Bacteriol* **2018**, *200*, e00014-00018, DOI: 10.1128/JB.00014-18.

18. Wadhwa, N.; Berg, H.C. Bacterial motility: machinery and mechanisms. *Nat Rev Microbiol* **2022**, *20*, 161-173, DOI: 10.1038/s41579-021-00626-4.

19. Daniels, R.; Reynaert, S.; Hoekstra, H.; Verreth, C.; Janssens, J.; Braeken, K.; Fauvart, M.; Beullens, S.; Heusdens, C.; Lambrichts, I., *et al.* Quorum signal molecules as biosurfactants affecting swarming in *Rhizobium etli*. *Proc Natl Acad Sci U S A* **2006**, *103*, 14965-14970, DOI: 10.1073/pnas.0511037103.

20. Tambalo, D.D.; Yost, C.K.; Hynes, M.F. Characterization of swarming motility in *Rhizobium leguminosarum* bv. *viciae*. *FEMS Microbiol Lett* **2010**, *307*, 165-174, DOI: 10.1111/j.1574-6968.2010.01982.x.

21. Covelli, J.M.; Althabegoiti, M.J.; López, M.F.; Lodeiro, A.R. Swarming motility in *Bradyrhizobium japonicum*. *Res Microbiol* **2013**, *164*, 136-144, DOI: 10.1016/j.resmic.2012.10.014.

22. Alías-Villegas, C.; Fuentes-Romero, F.; Cuéllar, V.; Navarro-Gómez, P.; Soto, M.J.; Vinardell, J.M.; Acosta-Jurado, S. Surface motility regulation of *Sinorhizobium fredii* HH103 by plant flavonoids and the NodD1, TtsI, NolR, and MucR1 symbiotic bacterial regulators. *Int J Mol Sci* **2022**, *23*, DOI: 10.3390/ijms23147698.

23. Holscher, T.; Kovacs, A.T. Sliding on the surface: bacterial spreading without an active motor. *Environ Microbiol* **2017**, *19*, 2537-2545, DOI: 10.1111/1462-2920.13741.

24. Mattick, J.S. Type IV pili and twitching motility. *Annu Rev Microbiol* **2002**, *56*, 289-314, DOI: 10.1146/annurev.micro.56.012302.160938.

25. Maier, B.; Wong, G.C.L. How bacteria use Type IV pili machinery on surfaces. *Trends Microbiol* **2015**, *23*, 775-788, DOI: 10.1016/j.tim.2015.09.002.

26. Pelicic, V. Type IV pili: *e pluribus unum*? *Mol Microbiol* **2008**, *68*, 827-837, DOI: 10.1111/j.1365-2958.2008.06197.x.

27. Craig, L.; Forest, K.T.; Maier, B. Type IV pili: dynamics, biophysics and functional consequences. *Nat Rev Microbiol* **2019**, *17*, 429-440, DOI: 10.1038/s41579-019-0195-4.

28. Denise, R.; Abby, S.S.; Rocha, E.P.C. Diversification of the type IV filament superfamily into machines for adhesion, protein secretion, DNA uptake, and motility. *PLoS Biol* **2019**, *17*, e3000390, DOI: 10.1371/journal.pbio.3000390.

29. Ellison, C.K.; Whitfield, G.B.; Brun, Y.V. Type IV Pili: dynamic bacterial nanomachines. *FEMS Microbiol Rev* **2022**, *46*, DOI: 10.1093/femsre/fuab053.

30. Ellison, C.K.; Kan, J.; Dillard, R.S.; Kysela, D.T.; Ducret, A.; Berne, C.; Hampton, C.M.; Ke, Z.; Wright, E.R.; Biais, N., *et al.* Obstruction of pilus retraction stimulates bacterial surface sensing. *Science* **2017**, *358*, 535-538, DOI: 10.1126/science.aan5706.

31. Giltner, C.L.; Nguyen, Y.; Burrows, L.L. Type IV pilin proteins: versatile molecular modules. *Microbiol Mol Biol Rev* **2012**, *76*, 740-772, DOI: 10.1128/MMBR.00035-12.

32. Kachlany, S.C.; Planet, P.J.; Bhattacharjee, M.K.; Kollia, E.; DeSalle, R.; Fine, D.H.; Figurski, D.H. Nonspecific adherence by *Actinobacillus actinomycetemcomitans* requires genes widespread in bacteria and archaea. *J Bacteriol* **2000**, *182*, 6169-6176, DOI: 10.1128/JB.182.21.6169-6176.2000.

33. Kachlany, S.C.; Planet, P.J.; DeSalle, R.; Fine, D.H.; Figurski, D.H. Genes for tight adherence of *Actinobacillus actinomycetemcomitans*: from plaque to plague to pond scum. *Trends Microbiol* **2001**, *9*, 429-437, DOI: 10.1016/s0966-842x(01)02161-8.

34. Kachlany, S.C.; Planet, P.J.; Desalle, R.; Fine, D.H.; Figurski, D.H.; Kaplan, J.B. *flp-1*, the first representative of a new pilin gene subfamily, is required for non-specific adherence of *Actinobacillus actinomycetemcomitans*. *Mol Microbiol* **2001**, *40*, 542-554, DOI: 10.1046/j.1365-2958.2001.02422.x.

35. Tomich, M.; Planet, P.J.; Figurski, D.H. The *tad* locus: postcards from the widespread colonization island. *Nat Rev Microbiol* **2007**, *5*, 363-375, DOI: 10.1038/nrmicro1636.

36. Roux, N.; Spagnolo, J.; de Bentzmann, S. Neglected but amazingly diverse type IVb pili. *Res Microbiol* **2012**, *163*, 659-673, DOI: 10.1016/j.resmic.2012.10.015.

37. Skerker, J.M.; Shapiro, L. Identification and cell cycle control of a novel pilus system in *Caulobacter crescentus*. *EMBO J* **2000**, *19*, 3223-3234, DOI: 10.1093/emboj/19.13.3223.

38. Wang, Y.; Haitjema, C.H.; Fuqua, C. The Ctp type IVb pilus locus of *Agrobacterium tumefaciens* directs formation of the common pili and contributes to reversible surface attachment. *J Bacteriol* **2014**, *196*, 2979-2988, DOI: 10.1128/JB.01670-14.

39. Tomich, M.; Fine, D.H.; Figurski, D.H. The TadV protein of *Actinobacillus actinomycetemcomitans* is a novel aspartic acid prepilin peptidase required for maturation of the Flp1 pilin and TadE and TadF pseudopilins. *J Bacteriol* **2006**, *188*, 6899-6914, DOI: 10.1128/JB.00690-06.

40. Tassinari, M.; Rudzite, M.; Filloux, A.; Low, H.H. Assembly mechanism of a Tad secretion system secretin-pilotin complex. *Nat Commun* **2023**, *14*, 5643, DOI: 10.1038/s41467-023-41200-1.

41. Xu, Q.; Christen, B.; Chiu, H.J.; Jaroszewski, L.; Klock, H.E.; Knuth, M.W.; Miller, M.D.; Elsliger, M.A.; Deacon, A.M.; Godzik, A., *et al.* Structure of the pilus assembly protein TadZ from *Eubacterium rectale*: implications for polar localization. *Mol Microbiol* **2012**, *83*, 712-727, DOI: 10.1111/j.1365-2958.2011.07954.x.

42. Perez-Cheeks, B.A.; Planet, P.J.; Sarkar, I.N.; Clock, S.A.; Xu, Q.; Figurski, D.H. The product of *tadZ*, a new member of the *parA/minD* superfamily, localizes to a pole in *Aggregatibacter actinomycetemcomitans*. *Mol Microbiol* **2012**, *83*, 694-711, DOI: 10.1111/j.1365-2958.2011.07955.x.

43. Clock, S.A.; Planet, P.J.; Perez, B.A.; Figurski, D.H. Outer membrane components of the Tad (tight adherence) secreton of *Aggregatibacter actinomycetemcomitans*. *J Bacteriol* **2008**, *190*, 980-990, DOI: 10.1128/JB.01347-07.

44. Seef, S.; Herrou, J.; de Boissier, P.; My, L.; Brasseur, G.; Robert, D.; Jain, R.; Mercier, R.; Cascales, E.; Habermann, B.H., *et al.* A Tad-like apparatus is required for contact-dependent prey killing in predatory social bacteria. *eLife* **2021**, *10*, DOI: 10.7554/eLife.72409.

45. Wairuri, C.K.; van der Waals, J.E.; van Schalkwyk, A.; Theron, J. *Ralstonia solanacearum* needs Flp pili for virulence on potato. *Mol Plant Microbe Interact* **2012**, *25*, 546-556, DOI: 10.1094/MPMI-06-11-0166.

46. Nykyri, J.; Mattinen, L.; Niemi, O.; Adhikari, S.; Kõiv, V.; Somervuo, P.; Fang, X.; Auvinen, P.; Mäe, A.; Palva, E.T., *et al.* Role and regulation of the Flp/Tad pilus in the virulence of *Pectobacterium atrosepticum* SCRI1043 and *Pectobacterium wasabiae* SCC3193. *PLOS ONE* **2013**, *8*, e73718, DOI: 10.1371/journal.pone.0073718.

47. Andrade, M.; Wang, N. The Tad Pilus Apparatus of '*Candidatus* Liberibacter asiaticus' and Its Regulation by VisNR. *Mol Plant Microbe Interact* **2019**, *32*, 1175-1187, DOI: 10.1094/MPMI-02-19-0052-R.

48. Vesper, S.J.; Bauer, W.D. Role of Pili (Fimbriae) in Attachment of *Bradyrhizobium japonicum* to Soybean Roots. *Appl Environ Microbiol* **1986**, *52*, 134-141, DOI: 10.1128/aem.52.1.134-141.1986.

49. Krehenbrink, M.; Downie, J.A. Identification of protein secretion systems and novel secreted proteins in *Rhizobium leguminosarum* bv. *viciae*. *BMC Genomics* **2008**, *9*, 55, DOI: 10.1186/1471-2164-9-55.

50. Mongiardini, E.J.; Parisi, G.D.; Quelas, J.I.; Lodeiro, A.R. The tight-adhesion proteins TadGEF of *Bradyrhizobium diazoefficiens* USDA 110 are involved in cell adhesion and infectivity on soybean roots. *Microbiol Res* **2016**, *182*, 80-88, DOI: 10.1016/j.micres.2015.10.001.

51. Schmeisser, C.; Liesegang, H.; Krysciak, D.; Bakkou, N.; Le Quere, A.; Wollherr, A.; Heinemeyer, I.; Morgenstern, B.; Pommerening-Roser, A.; Flores, M., *et al.* *Rhizobium* sp. strain NGR234 possesses a remarkable number of secretion systems. *Appl Environ Microbiol* **2009**, *75*, 4035-4045, DOI: 10.1128/AEM.00515-09.

52. Wibberg, D.; Blom, J.; Jaenicke, S.; Kollin, F.; Rupp, O.; Scharf, B.; Schneiker-Bekel, S.; Sczcepanowski, R.; Goesmann, A.; Setubal, J.C., *et al.* Complete genome sequencing of *Agrobacterium* sp. H13-3, the former *Rhizobium lupini* H13-3, reveals a tripartite genome consisting of a circular and a linear chromosome and an accessory plasmid but lacking a tumor-inducing Ti-plasmid. *J Biotechnol* **2011**, *155*, 50-62, DOI: 10.1016/j.jbiotec.2011.01.010.

53. Zatakia, H.M.; Nelson, C.E.; Syed, U.J.; Scharf, B.E. ExpR coordinates the expression of symbiotically important, bundle-forming Flp pili with quorum sensing in *Sinorhizobium meliloti*. *Appl Environ Microbiol* **2014**, *80*, 2429-2439, DOI: 10.1128/AEM.04088-13.

54. Casadesús, J.; Olivares, J. Rough and fine linkage mapping of the *Rhizobium meliloti* chromosome. *Mol Gen Genet* **1979**, *174*, 203-209, DOI: 10.1007/BF00268356.

55. Bellabarba, A.; Bacci, G.; Decorosi, F.; Aun, E.; Azzarello, E.; Remm, M.; Giovannetti, L.; Viti, C.; Mengoni, A.; Pini, F. Competitiveness for Nodule Colonization in *Sinorhizobium meliloti*: Combined In Vitro-Tagged

20

Strain Competition and Genome-Wide Association Analysis. *mSystems* **2021**, *6*, e0055021, DOI: 10.1128/mSystems.00550-21.

56. Schlüter, J.P.; Reinkensmeier, J.; Barnett, M.J.; Lang, C.; Krol, E.; Giegerich, R.; Long, S.R.; Becker, A. Global mapping of transcription start sites and promoter motifs in the symbiotic alpha-proteobacterium *Sinorhizobium meliloti* 1021. *BMC Genomics* **2013**, *14*, 156, DOI: 10.1186/1471-2164-14-156.

57. Christen, M.; Beusch, C.; Bösch, Y.; Cerletti, D.; Flores-Tinoco, C.E.; Del Medico, L.; Tschan, F.; Christen, B. Quantitative Selection Analysis of Bacteriophage φCbK Susceptibility in *Caulobacter crescentus*. *J Mol Biol* **2016**, *428*, 419-430, DOI: 10.1016/j.jmb.2015.11.018.

58. Mignolet, J.; Panis, G.; Viollier, P.H. More than a Tad: spatiotemporal control of *Caulobacter* pili. *Curr Opin Microbiol* **2018**, *42*, 79-86, DOI: 10.1016/j.mib.2017.10.017.

59. Hayashi, S.; Wu, H.C. Lipoproteins in bacteria. *J Bioenerg Biomembr* **1990**, *22*, 451-471, DOI: 10.1007/BF00763177.

60. Kaushik, S.; He, H.; Dalbey, R.E. Bacterial Signal Peptides- Navigating the Journey of Proteins. *Front Physiol* **2022**, *13*, DOI: 10.3389/fphys.2022.933153.

61. DAndrea, L.D.; Regan, L. TPR proteins: the versatile helix. *Trends Biochem Sci* **2003**, *28*, 655-662, DOI: 10.1016/j.tibs.2003.10.007.

62. Sangermani, M.; Hug, I.; Sauter, N.; Pfohl, T.; Jenal, U. Tad Pili Play a Dynamic Role in *Caulobacter crescentus* Surface Colonization. *MBio* **2019**, *10*, DOI: 10.1128/mBio.01237-19.

63. Turnbull, L.; Whitchurch, C.B. Motility Assay: Twitching Motility. In *Pseudomonas Methods and Protocols*, Filloux, A.; Ramos, J.-L., Eds. Springer New York: New York, NY, 2014; pp 73-86, ISBN. 978-1-4939-0473-0.

64. Duong-Nu, T.M.; Jeong, K.; Hong, S.H.; Puth, S.; Kim, S.Y.; Tan, W. A stealth adhesion factor contributes to *Vibrio vulnificus* pathogenicity: Flp pili play roles in host invasion, survival in the blood stream and resistance to complement activation. *PLoS Pathog* **2019**, *15*, e1007767, DOI: 10.1371/journal.ppat.1007767.

65. de Bentzmann, S.; Aurouze, M.; Ball, G.; Filloux, A. FppA, a novel *Pseudomonas aeruginosa* prepilin peptidase involved in assembly of type IVb pili. *J Bacteriol* **2006**, *188*, 4851-4860, DOI: 10.1128/JB.00345-06.

66. Kilmury, S.L.N.; Burrows, L.L. The *Pseudomonas aeruginosa* PilSR Two-Component System Regulates Both Twitching and Swimming Motilities. *mBio* **2018**, *9*, e01310-01318, DOI: 10.1128/mBio.01310-18.

67. Ellison, C.K.; Rusch, D.B.; Brun, Y.V. Flagellar Mutants Have Reduced Pilus Synthesis in *Caulobacter crescentus*. *J Bacteriol* **2019**, *201*, DOI: 10.1128/JB.00031-19.

68. Kühn, M.J.; Talà, L.; Inclan, Y.F.; Patino, R.; Pierrat, X.; Vos, I.; Al-Mayyah, Z.; Macmillan, H.; Negrete, J., Jr.; Engel, J.N., *et al.* Mechanotaxis directs *Pseudomonas aeruginosa* twitching motility. *Proc Natl Acad Sci U S A* **2021**, *118*, e2101759118, DOI: 10.1073/pnas.2101759118.

69. Laventie, B.J.; Jenal, U. Surface Sensing and Adaptation in Bacteria. *Annu Rev Microbiol* **2020**, *74*, 735-760, DOI: 10.1146/annurev-micro-012120-063427.

70. Del Medico, L.; Cerletti, D.; Schachle, P.; Christen, M.; Christen, B. The type IV pilin PilA couples surface attachment and cell-cycle initiation in *Caulobacter crescentus*. *Proc Natl Acad Sci U S A* **2020**, *117*, 9546-9553, DOI: 10.1073/pnas.1920143117.

71. Sambrook, J., Fritsch, E. F. & Maniatis, T. *Molecular Cloning: A Laboratory Manual*. Cold Spring Harbor Laboratory Press: Cold Spring Harbor, NY, 1989,

72. Beringer, J.E. R factor transfer in *Rhizobium leguminosarum*. *J Gen Microbiol* **1974**, *84*, 188-198, DOI: 10.1099/00221287-84-1-188.

73. Robertsen, B.K.; Aiman, P.; Darwill, A.G.; Mcneil, M.; Albersheim, P. The structure of acidic extracellular polysaccharides secreted by *Rhizobium leguminosarum* and *Rhizobium trifolii*. *Plant Physiol* **1981**, *67*, 389-400, DOI: 10.1104/pp.67.3.389.

74. Aziz, R.K.; Bartels, D.; Best, A.A.; DeJongh, M.; Disz, T.; Edwards, R.A.; Formsma, K.; Gerdes, S.; Glass, E.M.; Kubal, M., *et al.* The RAST Server: rapid annotations using subsystems technology. *BMC Genomics* **2008**, *9*, 75, DOI: 10.1186/1471-2164-9-75.

75. Kanehisa, M.; Sato, Y.; Kawashima, M.; Furumichi, M.; Tanabe, M. KEGG as a reference resource for gene and protein annotation. *Nucleic Acids Res* **2016**, *44*, D457-462, DOI: 10.1093/nar/gkv1070.

76. Olson, R.D.; Assaf, R.; Brettin, T.; Conrad, N.; Cucinell, C.; Davis, J.J.; Dempsey, D.M.; Dickerman, A.; Dietrich, E.M.; Kenyon, R.W., *et al.* Introducing the Bacterial and Viral Bioinformatics Resource Center (BV-BRC): a resource combining PATRIC, IRD and ViPR. *Nucleic Acids Res* **2023**, *51*, D678-D689, DOI: 10.1093/nar/gkac1003.

77. Paysan-Lafosse, T.; Blum, M.; Chuguransky, S.; Grego, T.; Pinto, B.L.; Salazar, G.A.; Bileschi, M.L.; Bork, P.; Bridge, A.; Colwell, L., *et al.* InterPro in 2022. *Nucleic Acids Res* **2023**, *51*, D418-D427, DOI: 10.1093/nar/gkac993.

78. Simon, R.; Priefer, U.; Pühler, A. A broad host range mobilization system for *in vivo* genetic-engineering: transposon mutagenesis in Gram-negative bacteria. *Nat Biotechnol* **1983**, *1*, 784-791, DOI: 10.1038/nbt1183-784.

79. Schäfer, A.; Tauch, A.; Jager, W.; Kalinowski, J.; Thierbach, G.; Pühler, A. Small mobilizable multi-purpose cloning vectors derived from the *Escherichia coli* plasmids pK18 and pK19: selection of defined deletions in the chromosome of *Corynebacterium glutamicum*. *Gene* **1994**, *145*, 69-73, DOI: 10.1016/0378-1119(94)90324-7.

80. Calatrava-Morales, N.; Nogales, J.; Ameztoy, K.; van Steenbergen, B.; Soto, M.J. The NtrY/NtrX System of *Sinorhizobium meliloti* GR4 Regulates Motility, EPS I Production, and Nitrogen Metabolism but Is Dispensable for Symbiotic Nitrogen Fixation. *Mol Plant Microbe Interact* **2017**, *30*, 566-577, DOI: 10.1094/mpmi-01-17-0021-r.

81. López-Lara, I.M.; Nogales, J.; Pech-Canul, A.; Calatrava-Morales, N.; Bernabéu-Roda, L.M.; Durán, P.; Cuéllar, V.; Olivares, J.; Alvarez, L.; Palenzuela-Bretones, D., *et al.* 2-Tridecanone impacts surface-associated bacterial behaviours and hinders plant-bacteria interactions. *Environ Microbiol* **2018**, *20*, 2049-2065, DOI: 10.1111/1462-2920.14083.

82. Olivares, J.; Casadesús, J.; Bedmar, E.J. Method for Testing Degree of Infectivity of *Rhizobium meliloti* Strains. *Appl Environ Microbiol* **1980**, *39*, 967-970, DOI: 10.1128/aem.39.5.967-970.1980.

83. García-Rodríguez, F.M.; Toro, N. *Sinorhizobium meliloti nfe* (nodulation formation efficiency) genes exhibit temporal and spatial expression patterns similar to those of genes involved in symbiotic nitrogen fixation. *Mol Plant Microbe Interact* **2000**, *13*, 583-591, DOI: 10.1094/MPMI.2000.13.6.583.